The Astrophysical Journal, Submitted 2003 February 13

THE r-PROCESS IN SUPERNOVA EXPLOSIONS FROM THE COLLAPSE OF O-Ne-Mg CORES

Shinya Wanajo, Masaya Tamamura, and Naoki Itoh

Department of Physics, Sophia University, 7-1 Kioi-cho, Chiyoda-ku, Tokyo, 102-8554, Japan;
wanajo@sophia.ac.jp, m-tamamu@sophia.ac.jp, n_itoh@sophia.ac.jp

Ken'ichi Nomoto

Department of Astronomy, School of Science, University of Tokyo, Bunkyo-ku, Tokyo, 113-0033, Japan; nomoto@astron.s.u-tokyo.ac.jp

Yuhri Ishimaru

Department of Physics and Graduate School of Humanities and Sciences, Ochanomizu University, 2-1-1 Otsuka, Bunkyo-ku, Tokyo 112-8610, Japan;
ishimaru@phys.ocha.ac.jp

Timothy C. Beers

Department of Physics/Astronomy, Michigan State University, E. Lansing, MI 48824, USA; beers@pa.msu.edu

and

Satoshi Nozawa

Josai Junior College for Women, 1-1 Keyakidai, Sakado-shi, Saitama, 350-0290, Japan;
snozawa@venus.josai.ac.jp

The Astrophysical Journal, Submitted 2003 February 13

ABSTRACT

While the origin of r-process nuclei remains a long-standing mystery, recent spectroscopic studies of extremely metal-poor stars in the Galactic halo strongly suggest that it is associated with core-collapse supernovae. In this study we examine r-process nucleosynthesis in a "prompt supernova explosion" from an $8-10M_{\odot}$ progenitor star, as an alternative scenario to the "neutrino wind" mechanism, which has also been considered to be a promising site of the r-process. In the present model, the progenitor star has formed an oxygen-neon-magnesium core (of mass $1.38M_{\odot}$) at its center. Its smaller gravitational potential, as well as the smaller core that is in nuclear statistical equilibrium at the time of core bounce, as compared to the iron cores in more massive stars, may allow the star to explode hydrodynamically, rather than by delayed neutrino heating. The core-collapse simulations are performed with a one-dimension, Newtonian hydrodynamic code. We obtain a very weak prompt explosion, in which no r-processing occurs. We further simulate energetic prompt explosions by enhancement of the shock-heating energy, in order to investigate conditions necessary for the production of r-process nuclei in such events. The r-process nucleosynthesis is calculated using a nuclear reaction network code including relevant neutron-rich isotopes with reactions among them. The highly neutronized ejecta ($Y_e \approx 0.14 - 0.20$) leads to robust production of r-process nuclei; their relative abundances are in excellent agreement with the solar r-process pattern. Our results suggest that prompt explosions of $8-10M_{\odot}$ stars with oxygen-neon-magnesium cores can be a promising site of r-process nuclei. The mass of the r-process material per event is about two orders of magnitude larger than that expected from Galactic chemical evolution studies. We propose, therefore, that only a small fraction of r-process material is ejected, owing to the "mixing-fallback" mechanism of the core matter, wherein most of the r-process material falls back onto the proto-neutron star.

A lower limit on the age of the universe is derived by application of the U-Th chronometer pair by comparison with the observed ratio of these species in the highly r-process enhanced, extremely metal-poor star CS 31082-001. The inferred age is 14.1 ± 2.4 Gyr – the same as that obtained previously based on the neutrino wind scenario with the same nuclear mass formula. This suggests that chronometric estimates obtained using the U-Th pair are independent of the astrophysical conditions considered.

Subject headings: nuclear reactions, nucleosynthesis, abundances — stars: abundances — supernovae: general

1. INTRODUCTION

The astrophysical origin of the rapid neutron-capture (r-process) species has been a long-standing mystery. Recently, however, a number of important new clues have been provided by spectroscopic studies of extremely-metal-poor stars in the Galaxy. The appearance of neutron-capture elements in these oldest stars in the Galaxy, including the pure-r-process origin of elements such as thorium and uranium, strongly suggests that the r-process nuclei have come from core-collapse supernovae (Sneden et al. 1996, 2000, 2003; Cayrel et al. 2001; Cowan et al. 2002; Hill et al. 2002). Ishimaru & Wanajo (1999) have shown that the large star-to-star dispersion of the observed abundances of neutron-capture elements relative to iron in very metal-poor stars is also naturally explained if the r-process elements originate from a limited mass range of core-collapse supernovae with little iron production ($8-10M_{\odot}$ or $\geq 30M_{\odot}$). Qian & Wasserburg (2003; see also Wasserburg & Qian 2000; Qian & Wasserburg 2001, 2002) have proposed that the production of the heavy r-process nuclei ($A > 130$) is decoupled from the production of iron-peak and α nuclei by comparison of observed abundances among the extremely metal-poor stars. In this view, the production site of the heavy r-process nuclei is associated with the accretion-induced collapse (AIC) of a (carbon-oxygen or oxygen-neon-magnesium) white dwarf in a binary system (Nomoto & Kondo 1991), or Type II supernovae from $8-10M_{\odot}$ stars (Nomoto 1984).

So far, the "neutrino wind" scenario, in which the free nucleons accelerated by the intense neutrino flux near the neutrino sphere of a core-collapse supernova assemble to heavier nuclei, has been believed to be the most promising astrophysical site of the r-process (Woosley et al. 1994). Even this scenario, however, encounters some difficulties (Qian & Woosley 1996; Hoffman et al. 1997; Cardall & Fuller 1997; Otsuki et al. 2000; Thompson, Burrows, & Meyer 2001; Wanajo et al. 2001, 2002). For example, Wanajo et al. (2001) have shown that an extremely compact proto-neutron star, e.g., $2.0M_{\odot}$ and 10 km, must be formed in order to account for the solar r-process pattern, at least within the framework of a spherically symmetric explosion. Although its possibility cannot be excluded, such a compact remnant is allowed by only a few of the many existing equations of state of nuclear matter.

In addition, recent spectroscopic studies of extremely metal-poor stars in the Galactic halo indicate that the observed abundance patterns of the lighter ($Z < 56$) and heavier ($Z > 56$) neutron-capture elements cannot be explained by a single astrophysical site (e.g., neutrino winds); there must exist at least two different r-process sites (Ishimaru & Wanajo 2000; Qian & Wasserburg 2001; Johnson & Bolte 2002; Sneden & Cowan 2003). Hence, it is of special importance to consider alternative possibilities for the occurrence of the r-process in core-collapse supernovae.

Nomoto (1984, 1987) has shown that $8-10M_{\odot}$ stars form an electron-degenerate oxygen-

neon-magnesium (O-Ne-Mg) core that does not undergo further nuclear burning; rather, it directly collapses due to electron capture on ^{24}Mg and ^{20}Ne (Miyaji et al. 1980). Hillebrandt, Nomoto, & Wolff (1984) have demonstrated that the collapsing O-Ne-Mg core explodes in a prompt manner, and Wheeler, Cowan, & Hillebrandt (1998) have suggested that the exploding O-Ne-Mg core could be a viable site for the r-process. It has been pointed out that, if the core exploded hydrodynamically prior to the onset of delayed neutrino heating (i.e., it underwent a prompt explosion), the electron fraction (electron number per baryon), Y_e, in the innermost layer of the ejecta would approach ~ 0.2 (Hillebrandt, Nomoto, & Wolff 1984). Earlier works have in fact shown that a robust r-process proceeds in such conditions (Schramm 1973; Sato 1974; Hillebrandt, Takahashi, & Kodama 1976).

Recently, Sumiyoshi et al. (2001) have demonstrated that the prompt explosion of an $11M_\odot$ star with an iron core might also be a promising site of the r-process. They obtained a prompt explosion by an adiabatic core-collapse calculation without inclusion of electron capture and neutrino transport. Thompson, Burrows, & Pinto (2003) have shown, however, that no explosion is obtained with such a progenitor (Woosley & Weaver 1995), when including electron capture along with a detailed treatment of neutrino transport. Many previous works have suggested that even the lowest mass of core-collapse supernovae ($\sim 10M_\odot$), in which a relatively smaller iron core is formed, may have difficulties in achieving a hydrodynamic explosion (Bowers & Wilson 1982; Burrows & Lattimer 1983, 1985; Bruenn 1989a,b; Baron & Cooperstein 1990).

On the other hand, the question of whether $8-10M_\odot$ stars that form O-Ne-Mg cores can explode hydrodynamically is still open. The possibility that these stars explode promptly remains because of the smaller iron core present at the onset of the core bounce, as well as the smaller gravitational potential of their collapsing cores. Hillebrandt, Nomoto, & Wolff (1984) have obtained a prompt explosion of a $9M_\odot$ star with a $1.38M_\odot$ O-Ne-Mg core, while others, using the same progenitor, have not (Burrows & Lattimer 1985; Baron, Cooperstein, & Kahana 1987). Mayle & Wilson (1988) obtained an explosion, not by a prompt shock, but by late-time neutrino heating. Similar results can be seen in the studies of AICs. Note that an AIC is an analogous phenomenon to a collapsing O-Ne-Mg core resulted from a single $8-10M_\odot$ star, since both consist of electron degenerate cores (Nomoto & Kondo 1991). Fryer et al. (1999) have obtained an explosion by neutrino heating, while others have not (Baron et al. 1987; Woosley & Baron 1992). The reason for these different outcomes is due, perhaps, to the application of different equations of state for dense matter, although other physical inputs may also have some influence (Fryer et al. 1999). Thus, even if a star of $8-10M_\odot$ exploded, it would be difficult to derive, with confidence, the physical properties as well as the mass of the ejected matter. Given this highly uncertain situation it is necessary to examine the resulting r-process nucleosynthesis in explosions obtained with different sets

of input physics.

The purpose of this study is to investigate conditions necessary for the production of r-process nuclei obtained in purely hydrodynamical models of prompt explosions of collapsing O-Ne-Mg cores, and to explore some of the consequences if those conditions are met. The core collapse and the subsequent core bounce are simulated by a one-dimensional hydrodynamic code with Newtonian gravity (§ 2). For simplicity, neutrino transport is not taken into account. Hence, we focus on only hydrodynamical explosions just after core bounce, not on the delayed explosions obtained via late-time neutrino heating. As seen in § 2, the explosion is marginal, and no r-processing is expected. In order to obtain r-processed material, we find it necessary to force the occurrence of more energetic explosions. The energetic explosions are simulated by artificial enhancements of the shock-heating energy, rather than by application of different sets of input physics, for simplicity. The r-process nucleosynthesis in these explosions is then calculated with the use of a nuclear reaction network code (§ 3). The resulting contribution of the r-process material created in these simulations to the early chemical evolution of the Galaxy is discussed in § 4. The results of chronometric age dating, using the U-Th chronometer pair based on our nucleosynthesis results, is discussed in § 5. A summary and conclusions follow in § 6.

2. PROMPT EXPLOSION

A pre-supernova model of a $9M_\odot$ star is taken from Nomoto (1984), which forms a 1.38 $M_\odot$ O-Ne-Mg core near the end of its evolution (**?**, see also)]Miya80, Miya87, Nomo87. We link this core to a one-dimensional implicit Lagrangian hydrodynamic code with Newtonian gravity (Bowers & Wilson 1991). This core is modeled with a finely zoned mesh of 200 mass shells ($2 \times 10^{-2} M_\odot$ to $0.8 M_\odot$, $5 \times 10^{-3} M_\odot$ to $1.3 M_\odot$, and $5 \times 10^{-3} - 1 \times 10^{-7} M_\odot$ to the edge of the core).

The equation of state of nuclear matter (EOS) is taken from Shen et al. (1998), which is based on relativistic mean field theory. The equation of state for the electron and positron gas includes arbitrary relativistic pairs as well as arbitrary degeneracy. Electron and positron capture on nuclei, as well as on free nucleons, are included, along with the use of the up-to-date rates from Langanke & Martinez-Pinedo (2000). The capture is suppressed above the neutrino trapping density, taken to be 3×10^{11} g cm^{-3}, since the neutrino transport process is not taken into account in this study. This simplification may be appropriate, since neutrinos at the early epoch of the core bounce do not appear to make a significant correction to the entropy compared to that obtained from shock heating as shown by Hillebrandt, Nomoto, & Wolff (1984). The delayed neutrino heating may not significantly modify the

mass trajectories of the outgoing matter either, since the bulk of the ejecta are lifted to ~ 1000 km during the first few 100 ms from the onset of the core bounce (as shown below), which is far from the location of the neutrino sphere (a few tens of kilometers). It is evident, however, that an accurate treatment of neutrino transport will be needed to obtain accurate mass trajectories in future work.

Nuclear burning is implemented in a simplified manner. The composition of the O-Ne-Mg core is held fixed until the temperature in each zone reaches the onset of oxygen-burning, taken to be 2×10^9 K (Nomoto 1987), at which point the matter is assumed to be instantaneously in nuclear statistical equilibrium (NSE). The temperature is then calculated by including its nuclear energy release. It should be noted that we find a weak α-rich freezeout in the subsequent post-processing nucleosynthesis calculations (§ 3), owing to the entropy, $\sim 10N_Ak$, in the ejecta. This means that the outgoing ejecta are not in perfect NSE, which is assumed in our hydrodynamic calculations. An improvement that takes the non-NSE matter properly into account will be needed to obtain more accurate trajectories.

We begin the hydrodynamical computations with this pre-supernova model, which has a density of 4.4×10^{10} g cm^{-3} and temperature of 1.3×10^{10} K at its center. The inner $0.1M_\odot$ has already burned to NSE. As a result, the central Y_e is rather low, 0.37, owing to electron capture. The core bounce is initiated when ~ 90 ms has passed from the start of the calculation. At this time the NSE core contains only $1.0M_\odot$, which is significantly smaller than the cases of collapsing iron cores ($\gtrsim 1.3M_\odot$). The central density is 2.2×10^{14} g cm^{-3}, significantly lower than that of **?**)slightly above 3×10^{14} g cm^{-3}]Hill84, although the temperature ($= 2.1 \times 10^{10}$ K) and Y_e ($= 0.34$), are similar. This difference is perhaps due to the use of a relatively stiff EOS in this study.

We find that a very weak explosion results, with an ejected mass of $0.008M_\odot$ and an explosion energy of 2×10^{49} ergs (model Q0 in Table 1). The time variations of the radius, temperature, and density of each zone are displayed in Figure 1. The lowest Y_e in the outgoing ejecta is 0.45, where no r-processing is expected given the entropy of $\sim 10N_Ak$. This is in contrast to the very energetic explosions, with ejected masses of $0.2M_\odot$, explosion energies of 2×10^{51} ergs, and low Y_e of ~ 0.2 obtained by Hillebrandt, Nomoto, & Wolff (1984). This might be a consequence of the lower gravitational energy release owing to the EOS applied in this study.

In order to examine the possible operation of the r-process in the explosion of this model, we artificially obtain explosions with typical energies of $\sim 10^{51}$ ergs by application of a multiplicative factor ($f_{\rm shock}$) to the shock-heating term in the energy equation (models Q3, Q5, and Q6 in Table 1). We take this simplified approach in this study, since the main difference between our result and that by Hillebrandt, Nomoto, & Wolff (1984) appear to

be the lower central density in ours. If the inner core reached a higher density at the time of core bounce by applying, for example, a softer EOS, the matter would obtain higher shock-heating energy. This is clearly not a self-consistent approach, and a further study is needed to conclude whether such a progenitor star explodes or not, taking into account a more accurate treatment of neutrino transport, as well as with various sets of input physics (like EOSs). It should be emphasized, however, that our purpose in this paper is not to justify the prompt explosions of collapsing O-Ne-Mg cores, but to investigate the conditions necessary for the production of r-process nuclei from such an event *if it occurs*.

Table 1 lists the multiplicative factor applied to the shock-heating term ($f_{\rm shock}$), explosion energy ($E_{\rm exp}$), ejected mass ($M_{\rm ej}$), and minimum Y_e in the ejecta obtained for each model. Energetic explosions with $E_{\rm exp} > 10^{51}$ ergs are obtained for $f_{\rm shock} \geq 1.5$ (models Q5 and Q6), in which deeper neutronized zones are ejected by the prompt shock, as can be seen in Figure 2 (model Q6). This is in contrast to the weak explosions with $E_{\rm exp} \leq 10^{50}$ ergs (models Q0 and Q3), in which only the surface of the core blows off (Figure 1). Note that the remnant masses for models Q5 and Q6 are $1.19M_\odot$ and $0.94M_\odot$, respectively, which are significantly smaller than the typical neutron star mass of $\sim 1.4M_\odot$. We consider it likely that a mass of $\sim 1.4M_\odot$ is recovered by fallback of the once-ejected matter, as discussed in § 4.

In Figure 3 the electron fraction in the ejecta of each model is shown as a function of the ejected mass point, $M_{\rm ej}$. For models Q0 and Q3, Y_e decreases steeply with $M_{\rm ej}$, since the duration of electron capturing is long, owing to the slowly expanding ejecta (Figure 1). For models Q5 and Q6, on the other hand, Y_e decreases gradually with $M_{\rm ej}$, owing to the fast expansion of the outgoing ejecta. Nevertheless, the inner regions approach very low Y_e, 0.30 and 0.14 for models Q5 and Q6, respectively, owing to their rather high density ($\sim 10^{11}$ g cm^{-3}) at the time of core bounce (Figure 2). Note that, for model Q6, Y_e increases again for $M_{\rm ej} > 0.3M_\odot$. This is due to the fact that the positron capture on free neutrons overcomes the electron capture on free protons when the electron degeneracy becomes less effective in the high temperature matter. The innermost, slowly outgoing region suffers from this effect. This can be also seen in the results of Mayle & Wilson (1988), who obtained a neutrino-powered (not *prompt*) explosion with the same O-Ne-Mg core.

The minimum Y_e (≈ 0.40) in Mayle & Wilson (1988) is, however, significantly higher than ours. This is mainly due to neutrino capture on free nucleons, since the matter is driven by intense neutrino flux in their simulation. Y_e might increase further once nucleons begin to assemble into α particles and heavy nuclei (**?**, the "α-effect";)]Meye98. In the case of the prompt explosions considered here, however, these neutrino effects may not alter Y_e significantly. The reason is that the bulk of the ejecta are lifted to ~ 1000 km at the arrival

of the delayed neutrinos (a few 100 ms from the onset of the core bounce), at which the capture timescale of neutrinos on free nucleons is no less than a few seconds (**?**, see, e.g., eq. (1) in)]Qian97. The dynamical timescales of the outgoing mass shells in model Q6 at $T_9 = 1, 3, 5$, and 7 (after the core bounce), defined by $\tau_{\rm dyn} = |\rho/(d\rho/dt)|$, are shown in Figure 4. As can be seen, the dynamical timescale prior to the r-process phase ($T_9 \gtrsim 3$) is significantly smaller than that of neutrino interaction.

The trend of the $Y_e - M_{\rm ej}$ relation up to $M_{\rm ej} \sim 0.2 M_\odot$ is similar in models Q5 and Q6, although it is inverted at $M_{\rm ej} \sim 0.14 M_\odot$, owing to the slightly different contribution of the positron and electron capture on free nucleons (Figure 3). Hence, the $Y_e - M_{\rm ej}$ relation between the surface and the innermost layer of the ejecta is expected to be similar to that of model Q6, as long as the explosion is sufficiently energetic ($\gtrsim 10^{51}$ ergs). In the subsequent sections, therefore, we focus only on model Q6, which is taken to be representative of cases where r-process nucleosynthesis occurs. The ejected mass, $M_{\rm ej}$, is thus taken to be a free parameter, instead of simulating many other models by changing $f_{\rm shock}$. Note that the results by Hillebrandt, Nomoto, & Wolff (1984) and Sumiyoshi et al. (2001) are very similar to the cases with $M_{\rm ej} \sim 0.2 - 0.3 M_\odot$ in model Q6.

3. THE r-PROCESS

The yields of r-process nucleosynthesis species, adopting the model described in § 2 for the physical conditions, are obtained by application of an extensive nuclear reaction network code. The network consists of ~ 3600 species, all the way from single neutrons and protons up to the fermium isotopes ($Z = 100$). We include all relevant reactions, i.e., (n, γ), (p, γ), (α, γ), (p, n), (α, p), (α, n), and their inverses. Reaction rates are taken from Thielemann (1995, private communication) for nuclei with $Z \leq 46$ and from Cowan, Thielemann, & Truran (1991) for those with $Z \geq 47$. The latter used the mass formula by Hilf et al. (1976). The three-body reaction $\alpha(\alpha n, \gamma)^9$Be, which is of special importance as the bottleneck reaction to heavier nuclei, is taken from the recent experimental data of Utsunomiya et al. (2001). The weak interactions, such as β-decay, β-delayed neutron emission (up to three neutrons), and electron capture are also included, although the latter is found to be unimportant.

The α-decay chains and spontaneous fission processes are taken into account only after the freezeout of all other reactions, as in Wanajo et al. (2002). For the latter, all nuclei with $A \geq 256$ are assumed to decay by spontaneous fission only. The few known nuclei undergoing spontaneous fission for $A < 256$ are also included, along with their branching ratios. Neutron-induced and β-delayed fissions, as well as the contribution of fission fragments to the lighter nuclei, are neglected. Obviously, these treatments of the fission reactions are

oversimplified. Nevertheless, this may be acceptable, at least to first order. We leave more accurate treatment of these matters to future work.

Each calculation is started at $T_9 = 9$ (where $T_9 \equiv T/10^9$ K). The initial composition is taken to be that of NSE with the density and electron fraction at $T_9 = 9$, and consists mostly of free nucleons and alpha particles.

For reasons outlined in § 2, we examine the nucleosynthesis in model Q6 only, in which robust r-processing is expected. The resulted abundances in several representative Lagrangian mass shells are depicted in Figure 5. The initial electron fractions are 0.29, 0.20, 0.18, 0.16, 0.14, and 0.20 for the corresponding zone numbers 83, 92, 95, 98, 105, and 132, respectively. As can be seen, a robust r-processing is possible only for $Y_e \lesssim 0.20$. In particular, a substantial amount of thorium and uranium are produced only when Y_e is less than 0.18.

The mass-integrated abundances from the surface (zone 1) to the zones 83, 92, 95, 98, 105, and 132 are compared with the solar r-process abundances (Käppeler et al. 1989) in Figure 6 (models Q6a-f in Table 2). The latter is scaled to match the height of the first ($A = 80$) and third ($A = 195$) peaks of the abundances in models Q6a-b and Q6c-f, respectively. The ejecta masses of these models are listed in Table 2. The nucleosynthesis result in model Q5 (not presented here) is expected to be similar to that of model Q6a, because of the resemblance of the $Y_e - M_{\rm ej}$ profiles between these models (Figure 3). As can be seen in Figure 6, a solar r-process pattern for $A \gtrsim 130$ is naturally reproduced in models Q6c-f, while models Q6a-b fail to reproduce the third abundance peak. This implies that the region with $Y_e < 0.20$ must be ejected to account for production of the third r-process peak. Furthermore, to account for the solar level of thorium ($A = 232$) and uranium ($A = 235, 238$) production, the region with rather low Y_e (< 0.18) must be ejected. Note that large deficiencies of nuclei at $A \approx 115$ may be supplied if the slower rates of neutron capture in this region are adopted, as demonstrated by Goriely (1997).

We find that, for models Q6c-e, the lighter r-process nuclei with $A < 130$ are somewhat deficient compared to the solar r-process pattern (Figure 6c-e). This trend can be also seen in the observational abundance patterns of the highly r-process-enhanced, extremely metal- poor stars CS 22892-052 (Sneden et al. 2003) and CS 31082-001 (Hill et al. 2002). In model Q6f, the deficiency is outstanding because of large ejection of the low Y_e matter (Figure 3). This is in contrast to the previous results obtained for the neutrino wind scenario, which significantly *overproduce* the nuclei with $A \approx 90$ (Woosley et al. 1994; Wanajo et al. 2001). The nuclei with $A < 130$ can be supplied by slightly less energetic explosions, like models Q6a-b (Figures 5a-b). It is also possible to consider that these lighter r-process nuclei originate from "neutrino winds" in more massive supernovae ($> 10 M_\odot$). The nuclei with

$A < 130$ can be produced naturally in neutrino winds with a reasonable compactness of the proto-neutron star, e.g., $1.4M_\odot$ and 10 km (Wanajo et al. 2001).

Figure 6 implies that the production of thorium and uranium differs from model to model, even though the abundance pattern seems to be *universal* between the second and third r-process peaks, as seen in models Q6c-f. This is in agreement with recent observational results suggesting that the ratio Th/Eu may exhibit a star-to-star scatter, while the abundance pattern between the second and third peaks is in good agreement with the solar r-process pattern (Honda et al., in preparation). Thus, the use of Th/Eu as a cosmochronometer should be regarded with caution, at least until the possible variations can be better quantified; U/Th might be a far more reliable chronometer, as discussed further in § 5.

It is interesting to note that the nucleosynthesis results obtained for models Q6c-e are in good agreement with that of the prompt explosion of a $11M_\odot$ star with an iron core by Sumiyoshi et al. (2001). Our results seem, however, in better agreement with the solar r-process pattern, in particular near the rare-earth peak ($A \approx 160$) and the third peak ($A \approx 195$). This is a consequence of the slower ejection of the innermost region in our results owing to the reduction of pressure by electron capture, which is not taken into account in Sumiyoshi et al. (2001). In particular, the dynamical timescale of outgoing matter becomes significantly long during the epoch of the r-process ($T_9 \sim 3$ to 1), as can be seen in Figure 4. The extremely low Y_e (< 0.2) drives matter near the neutron-drip line, where the abundance pattern deviates from the solar one. In our models, however, the solar r-process pattern is recovered by the "freezeout effect" after the epoch of r-processing, as discussed in detail by Wanajo et al. (2002). This arises because the matter stays at higher temperatures for a longer time, hence the quasi-equilibrium between neutron emission by photodisintegration and subsequent neutron-capture processes continues to operate (Surman & Engel 2001).

It is also interesting to note that the mass of the r-processed ejecta in our results ($\gtrsim 0.05M_\odot$) is more than one order of magnitude larger than that obtained by **?**)$\sim 0.003M_\odot$]Sumi01. This is also a consequence of the longer dynamical timescale of outgoing ejecta in our simulation. The α particles are mostly consumed prior to the r-process phase in our calculations, whereas they dominate the final nucleosynthesis yields in Sumiyoshi et al. (2001). These results strongly suggest that an accurate treatment of electron capture, as well as of neutrino transport, will be crucial to derive an accurate prediction of the r-process abundances from prompt explosions of O-Ne-Mg cores.

4. CONTRIBUTION TO CHEMICAL EVOLUTION OF THE GALAXY

We have demonstrated in the previous section that, if stars of $8-10M_\odot$ do explode energetically, the solar r-process pattern can be reproduced quite naturally. It is of importance, however, to see if the nucleosynthetic material contributed to the Galaxy from such stars is consistent with the currently observed elemental abundances in the solar neighborhood.

Figure 7 shows the "production factors" per supernova for model Q6e, defined for each nuclide as the final mass fraction, $X_{\rm ej}$, diluted by the total ejected mass ($7.9M_\odot$) from the $9M_\odot$ star, divided by its solar abundance $X_\odot$ (Anders & Grevesse 1989). The solid lines connect isotopes of a given element (after nuclear decay). The dotted horizontal lines indicate a "normalization band" between the largest production factor (^{129}Xe) and that by a factor of ten less than that, along with a median value (dashed line). This band is taken to be representative of the uncertainty in the nuclear data for very neutron-rich nuclei (Woosley et al. 1994). As can be seen in Figure 7, a majority of the nuclei with $A > 100$ fall within the normalization band (except for the large deficiencies near $A = 120$), which is regarded to be the dominant species produced. The deficiencies near $A = 88, 138$, and 208 may be supplied by s-process contributions from other sources. Although such a supernova might be considered a likely production site of r-process nuclei, its contribution to nuclei with $A < 80$, including the α elements and iron-peak species, is negligible.

One of the essential questions raised by previous works is that, if prompt supernova explosions are one of the major sites of r-process nuclei, would in fact the r-process nuclei be significantly *overproduced* (Hillebrandt, Takahashi, & Kodama 1976). As far as the explosion is purely hydrodynamical, a highly neutronized deeper region must be ejected in order for a successful r-process to result. It seems inevitable, therefore, that one must avoid an ejection of large amounts of r-process matter, at least when assuming spherical symmetry. Our result shows that more than $0.05M_\odot$ of the r-process matter ($A \geq 120$) is ejected per event, which reproduces the solar r-process pattern (models Q6c-f in Table 2). This is about three orders of magnitude larger than the $5.8 \times 10^{-5}M_\odot$ in the neutrino-heated supernova ejecta from a $20M_\odot$ star obtained by Woosley et al. (1994). This value might would be reduced to some extent by α-rich freezeout in faster outgoing mass shells than ours as observed in Sumiyoshi et al. (2001). However, good agreement with the solar r-process pattern would not be achieved in the ejecta expanding too fast, as discussed in § 3.

As discussed by Woosley et al. (1994), production factors must be on the order of ~ 10 for the case that all supernovae contribute equally to r-process production in the Galaxy. Stars of $8-10M_\odot$ would account for $\sim 30\%$ of all supernovae (if they explode). The ejected masses ($\sim 7-9M_\odot$) are smaller than a factor of two to three than those from more massive supernovae. Thus, production factors of ~ 100 are allowed in the case that all $8-10M_\odot$

stars contribute equally to the Galactic r-process material. The production factors in our results are, however, about three orders of magnitude higher than this (Figure 7).

It might be argued that this type of event is extremely rare, accounting for only $0.01 - 0.1\%$ of all core-collapse supernovae. However, observations of extremely metal-poor stars ([Fe/H] ~ -3) in the Galactic halo show that at least two, CS 22892-052 and CS 31082-001, out of about a hundred studied at high resolution, imply contributions from highly r-process-enhanced supernova ejecta (Sneden et al. 2000; Hill et al. 2002). Moreover, such an extremely rare event would result in a much larger dispersion of r-process elements relative to iron than is currently observed amongst extremely metal-poor stars. Ishimaru & Wanajo (1999) demonstrated that the observed star-to-star dispersion of [Eu/Fe] over a range ~ -1 to 2 dex, was reproduced by their chemical evolution model if Eu originated from stars of $8 - 10 M_{\odot}$. Recent abundance measurements of Eu in a few extremely metal-poor stars with [Fe/H] $\lesssim -3$ by SUBARU/HDS further supports their result (Ishimaru et al., in preparation). The requisite mass of Eu in their model is $\sim 10^{-6} M_{\odot}$ per event. The ejected mass of Eu in our result is more than two orders of magnitude larger (Table 2).

In order to resolve this conflict, we propose that the "mixing-fallback" mechanism operates in this kind of supernova. The peculiar abundance patterns of some extremely iron-deficient stars, including HE 0107-5240 with [Fe/H] $= -5.3$ (Christlieb et al. 2002), is explained successfully with this mechanism, as proposed by Umeda & Nomoto (2002, 2003). If a substantial amount of the hydrogen and helium envelope remains at the onset of the explosion, the outgoing ejecta may undergo large-scale mixing by Rayleigh-Taylor instabilities, which is believed to have happened in SN1987A (Hachisu et al. 1990; Herant & Woosley 1994; Kifonidis et al. 2003). Thus a tiny amount, say, $\sim 1\%$, of the r-process material is mixed into the outer layers and then ejected, but most of the core material may fall back onto the proto-neutron star via the reverse shock arising from the hydrogen-helium layer interface. In this case, the typical mass of the proto-neutron star ($\sim 1.4 M_{\odot}$) is recovered. An asymmetric explosion mechanism, such as that which might arise from rotating cores, may have a similar effect as the ejection of deep-interior material in a small amount (Yamada & Sato 1994; Fryer & Heger 2000). This "mixing-fallback" scenario must be further tested by detailed multidimensional-hydrodynamic studies. However, it may provide us with a new paradigm for the nature of supernova nucleosynthesis.

This type of event may be characterized as a "faint" supernova, owing to the weakened explosion energy as well as the reduced amount of ^{56}Ni by "mixing-fallback". In addition, its ejecta consists mostly of hydrogen and helium with a higher ratio of He/H than that in the solar system. This event can be easily distinguished from the core-collapse supernovae of iron cores resulted from stars of $> 10 M_{\odot}$, which are characterized by abundant α-elements. It is

interesting to note that such an explosion bears a close resemblance to the Crab supernova, SN1054 (Nomoto et al. 1982). There is the possibility, therefore, that direct evidence will be obtained from the Crab nebula (or other similar supernova remnants) through the detection of r-process elements by future observations (Wallerstein et al. 1995). Detection of the γ-ray lines from decays of radioactive isotopes produced by the r-process could provide additional direct evidence for this scenario (Qian, Vogel, & Wasserburg 1998).

It is of special importance to confirm, from spectroscopic studies of extremely metal-poor stars in the Galactic halo, that the r-process elements are *not* associated with the production of α- and iron-peak elements (Wasserburg & Qian 2000; Qian & Wasserburg 2001, 2002). Qian & Wasserburg (2003) have suggested that the r-process enrichment in extremely metal-poor stars HD 115444, HD 122563, and CS 31082-001 is independent of the production of the elements from Na to Zn (including α- and iron-peak elements). The abundances of Na-Zn among these stars are mostly the same, while the level of r-process enhancement differs from star to star. These authors take this as evidence that the heavy r-process nuclei originated from AICs or Type II supernovae from $8 - 10 M_\odot$ stars, although they prefer AICs for the r-process site. Note that the nucleosynthetic outcome of an AIC event may be similar to the collapsing O-Ne-Mg core resulting from a single $8 - 10 M_\odot$ star. Hence, it is possible that AICs also undergo prompt explosions. The frequency of the AIC events in the Galaxy is expected to be very small, $\sim 10^{-5}$ yr^{-1} (Bailyn & Grindlay 1990). Assuming that the frequency of the core-collapse supernovae in the Galaxy is $\sim 10^{-2}$ yr^{-1} (Cappellaro et al. 1997), the production factor per AIC event is $\sim 10^4$. This is in reasonable agreement with our result of $\approx 10^5$, as can be seen in Figure 7. In the case of AICs, however, there is no chance to undergo "mixing-fallback", owing to the absence of the outer envelope. Thus, a much larger dispersion of [Eu/Fe] than that observed in the extremely metal-poor stars seems difficult to avoid.

We consider, therefore, that the heavy r-process nuclei originate from $8 - 10 M_\odot$ stars discussed in this study, being independent of whether they are single stars or are in binary systems. The lighter r-process elements ($Z < 56$) observed in extremely metal-poor stars may represent simply the interstellar medium from which these stars were formed, which originated from, perhaps, "neutrino winds" in supernovae from stars of $> 10 M_\odot$. The observed abundances of Eu relative to iron in extremely metal-poor stars are in fact well reproduced with this assumption in the chemical evolution model by Ishimaru & Wanajo (1999). Future spectroscopic studies of extremely metal-poor stars may be able to distinguish the scenario suggested in this study from AICs, for example, through observations of s-process abundances originating from mass transfer in binary systems.

5. U-Th COSMOCHRONOLOGY

The recently discovered r-process-enhanced, extremely metal-poor star, CS 31082-001 ([Fe/H] $= -2.9$) has provided a new, potentially quite powerful cosmochronometer, uranium (Cayrel et al. 2001; Hill et al. 2002). Wanajo et al. (2002) have determined the age of this star (more precisely, the time that has passed since the production event of the r-process species incorporated into this star) using the U-Th chronometer pair to be 14.1 ± 2.5 Gyr, based on the neutrino wind scenario. This is regarded as a hard lower limit of the age of the universe, and is in good agreement with that derived by an site-independent approach (Goriely & Arnould 2001; Schatz et al. 2002). It is of interest to examine if the same age of this star is also obtained, based on the prompt explosion model of a $9M_\odot$ star described in the previous sections. Note that the same mass formula (Hilf et al. 1976) as in Wanajo et al. (2002) is used in this study for comparison.

In Figure 8 the available spectroscopic abundance data for CS 31082-001 (dots) are compared with the nucleosynthesis result of model Q6e discussed in § 3 (thick line) and with the solar r-process pattern (thin line), scaled at Eu ($Z = 63$). The data for the neutron-capture elements in this star are taken from Hill et al. (2002). An overall agreement of our result with the spectroscopic data up to lead ($Z = 82$) can be seen, although our result appears somewhat deficient for the lighter elements. This is in contrast to the results in neutrino winds (Wanajo et al. 2002), in which the lighter elements are significantly overproduced. Thus, this model might be a reasonable one for the r-process events that produce large amounts of thorium and uranium, and whose products now appear in the atmosphere of CS 31082-001.

Figure 9 shows the mass-integrated abundance ratios of Th/Eu (open squares) and U/Th (open circles) from the surface to the mass point $M_{\rm ej}$, as well as the inferred ages of CS 31082-001, t^*(Th/Eu) (filled squares) and t^*(U/Th) (filled circles). As discussed by Hill et al. (2002), the age of CS 31082-001 can be inferred by application of the following relations:

$$t^*(\mathrm{Th/Eu}) = 46.67\,[\log(\mathrm{Th/Eu})_0 - \log(\mathrm{Th/Eu})_{\rm now}]\ \mathrm{Gyr} \quad (1)$$

$$t^*(\mathrm{U/Th}) = 21.76\,[\log(\mathrm{U/Th})_0 - \log(\mathrm{U/Th})_{\rm now}]\ \mathrm{Gyr} \quad (2)$$

where the half lives of ^{232}Th (14.05 Gyr) and ^{238}U (4.468 Gyr), and the subscripts "0" and "now" denote the initial and current values derived by theory and observation, respectively. In principle, t^*(U/Th) may serve as a more precise chronometer than t^*(Th/Eu), owing to the smaller coefficients in front of equations (2). Moreover, the ratio U/Th is less dependent on the model parameter $M_{\rm ej}$, since these species are separated by only two units in atomic number. Note that ^{235}U is assumed to have α-decayed away because of its relatively short half life (0.704 Gyr).

As can be seen in Figure 9, U/Th approaches a constant value (= 0.51) for $M_{\rm ej} \gtrsim 0.26 M_\odot$ ($Y_e \lesssim 0.17$), while Th/Eu varies widely. As a result, the age of CS 31082-001 determined by U/Th results in a constant value, t^*(U/Th) = 14.1 Gyr, for $M_{\rm ej} \gtrsim 0.26 M_\odot$. The age t^*(Th/Eu) is sensitive to the parameter $M_{\rm ej}$, ranging from a negative age to 23.8 Gyr, which illustrates that caution must be used in the application of this chronometer pair. It is useful, however, to take t^*(Th/Eu) as a constraint on the model parameter $M_{\rm ej}$, although the result might be changed if one includes an accurate neutrino transport and other input physics. It is found that the models with $M_{\rm ej} = 0.30 M_\odot$ and $0.37 M_\odot$ (zone numbers 105 and 118, respectively) give the same ages between t^*(Th/Eu) and t^*(U/Th). The former corresponds to model Q6e, which would provide a consistent scenario for the origin of the r-process elements in CS 31082-001, as can be seen in Figure 8. It should be noted that the fission fragments in model Q6e account for 23% of the mass contained in $A \geq 120$ nuclei (the last column in Table 2), whose contribution to the abundance pattern is neglected in this study. Obviously, more accurate treatment of fission reactions is needed. Nevertheless, the age t^*(U/Th) would not be altered significantly by this improvement, since the ratio U/Th is at the saturated value (= 0.51) at $M_{\rm ej} = 0.26 M_\odot$, where the mass fraction of fission fragments is only 2%.

It is noteworthy that the inferred age by U/Th in this study is the same as the result in Wanajo et al. (2002), which is based on a different astrophysical scenario (neutrino winds), but uses the same nuclear mass formula (Hilf et al. 1976). Our result confirms the robustness of the age determination using the U-Th chronometer pair, which is mostly independent of the astrophysical conditions considered. Rather than the r-process site, the nuclear mass formulae adopted, as well as the treatment of fission are crucial as far as the U-Th pair is concerned (Seeger & Schramm 1970; Goriely & Arnould 2001; Schatz et al. 2002).

6. SUMMARY AND CONCLUSIONS

We have examined the r-process nucleosynthesis obtained in the prompt explosion arising from the collapse of a $9 M_\odot$ star with an O-Ne-Mg core. The core collapse and subsequent core bounce were simulated with a one-dimensional, implicit, Lagrangian hydrodynamic code with Newtonian gravity. Neutrino transport was neglected for simplicity. We obtained a very weak explosion (model Q0) with an explosion energy of $\sim 2 \times 10^{49}$ ergs, and an ejected mass of $\sim 0.008 M_\odot$. No r-processing occurred in this model, because of the high electron fraction ($\gtrsim 0.45$) with low entropy ($\sim 10 N_A k$).

We further simulated energetic explosions by an artificial enhancement of the shock-heating energy, which might be expected from calculations with other sets of input physics, as

well as with other pre-supernova models. This resulted in an explosion energy of $\gtrsim 10^{51}$ ergs and an ejected mass of $\gtrsim 0.2 M_{\odot}$. Highly neutronized matter ($Y_e \approx 0.14$) was ejected, which led to strong r-processing (model Q6). Material arising from r-process nucleosynthesis was calculated with a nuclear reaction network code containing ~ 3600 isotopes with all relevant reactions. The result was in good agreement with the solar r-process pattern, in particular for nuclei with $A > 130$. Some of lighter r-process nuclei ($A < 130$) were deficient, which is consistent with the abundance patterns of the highly r-process enhanced, extremely metal-poor stars CS 22892-052 and CS 31082-001. This implies that the lighter r-process nuclei may originate from another site, which we suggest might be associated with the "neutrino wind" in core-collapsing supernovae of iron cores resulted from more massive stars ($> 10 M_{\odot}$).

The large ejection of r-process material ($\gtrsim 0.05 M_{\odot}$ per event) conflicts with the level of dispersion of r-process elements relative to iron observed in extremely metal-poor stars. We suggest, therefore, that only a small fraction ($\sim 1\%$) of the r-processed material is ejected, while the bulk of such material falls back onto the proto-neutron star by the "mixing-fallback" mechanism.

The age of the highly r-process enhanced, extremely metal-poor star, CS 31082-001 was derived by application of the U-Th chronometer pair, and can be regarded as a hard lower limit on the age of the universe. The age obtained is 14.1 ± 2.4 Gyr (the quoted error only includes that arising from the observations), the same as that based on a different astrophysical site, the neutrino-wind scenario (Wanajo et al. 2002), using the same nuclear mass formula. This confirms that the age determined by the U-Th pair is mostly independent of the astrophysical environment considered. The dependence of age dating on different nuclear mass formulae, based on the prompt explosion scenario presented in this paper, will be reported in future work.

It is obvious that more studies, including an accurate treatment of neutrino transport and other input physics, as well as multi-dimensional simulations of prompt supernova explosions, are needed to derive the final conclusion on the r-process scenario presented in this study. Nevertheless, this scenario is attractive as a promising site of the r-process, since the solar r-process pattern can be naturally reproduced without the problematic overproduction of $A \approx 90$ that appeared in the neutrino wind scenario. This type of event is characterized with the absence of α- and iron-peak elements, which can be easily distinguished from that of the core-collapsing iron core resulted from a more massive star ($> 10 M_{\odot}$). Future spectroscopic studies of extremely metal-poor stars in the Galactic halo will reveal if the collapsing O-Ne-Mg cores of $8 - 10 M_{\odot}$ stars are a viable site for the production of r-process nuclei. Improved observational determination of the U/Th ratio in CS 31082-001, as is presently being pursued, as well as a measured abundance of Pb in this star (as is being obtained

with the Hubble Space Telescope), and the identification of a greater number of highly r-process-enhanced, metal-poor stars, also underway, will surely deepen our understanding of the relevant processes involved.

We would like to acknowledge K. Sumiyoshi for providing an EOS table of nuclear matter applied in this study and for helpful discussions. We also thank G. Martinez-Pinedo for providing a data table of weak rates. We also acknowledge the contributions of an anonymous referee, which led to clarification of a number of points in our original presentation. This work was supported by a Grant-in-Aid for Scientific Research (13640245, 13740129, 14047206, 14540223) from the Ministry of Education, Culture, Sports, Science, and Technology of Japan. T.C.B. acknowledges partial support from grants AST 00-98508 and AST 00-98549 awarded by the U.S. National Science Foundation.

Table 1. Results of Core-Collapse Simulations

model	$f_{\rm shock}$	$E_{\rm exp}$ (10^{51} ergs)	$M_{\rm ej}$ ($M_\odot$)	$Y_{e,\rm min}$
Q0	1.0	0.018	0.0079	0.45
Q3	1.3	0.10	0.029	0.36
Q5	1.5	1.2	0.19	0.30
Q6	1.6	3.5	0.44	0.14

Table 2. Ejected Mass ($M_\odot$)

model	$M_{\rm ej}$	$A \geq 120$	^{56}Ni	Fe	Eu	fission†
Q0	0.0079	0.0	0.0018	0.0019	0.0	0.0
Q6a	0.19	2.6×10^{-4}	0.018	0.020	0.0	0.0
Q6b	0.24	0.035	0.018	0.020	2.4×10^{-4}	1.4×10^{-6}
Q6c	0.25	0.051	0.018	0.020	4.1×10^{-4}	4.3×10^{-4}
Q6d	0.27	0.064	0.018	0.020	4.3×10^{-4}	0.047
Q6e	0.30	0.080	0.018	0.020	4.6×10^{-4}	0.23
Q6f	0.44	0.21	0.018	0.020	0.0020	0.15

†mass fraction of fission fragments ($A \geq 120$)

REFERENCES

Anders, E., & Grevesse, N. 1989, Geochim. Cosmochim. Acta, 53, 197

Bailyn, C. D. & Grindlay, J. E. 1990, ApJ, 353, 159

Baron, E., Cooperstein, J., & Kahana, S. 1987, ApJ, 320, 300

Baron, E., Cooperstein, J., Kahana, S., & Nomoto, K. 1987, ApJ, 320, 304

Baron, E. & Cooperstein, J. 1990, ApJ, 353, 597

Bowers, R. & Wilson, J. R. 1982, ApJ, 263, 366

Bowers, R. & Wilson, J. R. 1991, Numerical Modeling in Applied Physics and Astrophysics (Jones and Bartlett)

Bruenn, S. W. 1989, ApJ, 340, 955

Bruenn, S. W. 1989, ApJ, 341, 385

Burrows, A. & Lattimer, J. M. 1983, ApJ, 270, 735

Burrows, A. & Lattimer, J. M. 1985, ApJ, 299, L19

Cappellaro, E., Turatto, M., Tsvetkov, D. Yu., Bartunov, O. S., Pollas, C., Evans, R., Hamuy, M. 1997, A&A, 322, 431

Cardall, C. Y. & Fuller, G. M. 1997, ApJ, 486, L111

Cayrel, R., Hill, V., Beers, T. C., Barbuy, B., Spite, M., Spite, F., Plez, B., Andersen, J., Bonifacio, P., Francois, P., Molaro, P., Nordstrom, B., & Primas, F. 2001, Nature, 409, 691

Christlieb, N., Bessell, M. S., Beers, T. C., Gustafsson, B., Korn, A., Barklem, P. S., Karlsson, T., Mizuno-Wiedner, M., & Rossi, S. 2002, Nature, 419, 904

Cowan, J. J., Thielemann, F. -K., & Truran, J. W. 1991, Phys. Rep., 208, 267

Cowan, J. J., Sneden, C., Burles, S., Ivans, I. I., Beers, T. C., Truran, J. W., Lawler, J. E., Primas, F., Fuller, G. M., Pfeiffer, B., & Kratz, K. -L. 2002, ApJ, 572, 861

Fryer, C., Benz, W., Herant, M., & Colgate, S. A. 1999, ApJ, 516, 892

Fryer, C. & Heger, A. 2000, ApJ, 541, 1033

Goriely, S. 1997, A&A, 325, 414

Goriely, S. & Arnould, M. 2001, A&A, 379, 1113

Hilf, E. R., von Groote, H., & Takahashi, K. 1976, in Proc. Third International Conference on Nuclei Far from Stability (Geneva: CERN), 142

Hachisu, I., Matsuda, T., Nomoto, K., & Shigeyama, T. 1990, ApJ, 358, L57

Herant, M. & Woosley, S. E. 1994, ApJ, 425, 814

Hill, V., Plez, B., Cayrel, R., Beers, T.C., Nordström, B., Andersen, J., Spite, M., Spite, F., Barbuy, B., Bonifacio, P., Depagne, E., François, P., Molaro, P., & Primas, F. 2002, A&A, 387, 560

Hillebrandt, W., Takahashi, K., & Kodama, T. 1976, A&A, 52, 63

Hillebrandt, W., Nomoto, K., & Wolff, G. 1984, A&A, 133, 175

Hoffman, R. D., Woosley, S. E., & Qian, Y. -Z. 1997, ApJ, 482, 951

Ishimaru, Y. & Wanajo, S. 1999, ApJ, 511, L33

Ishimaru, Y. & Wanajo, S. 2000, in First Stars, ed. A. Weiss, T. Abel,& V. Hill (Berlin: Springer), 189

Johnson, J. A. & Bolte, M. 2002, ApJ, 579, 616

Käppeler, F., Beer, H., & Wisshak, K. 1989, Rep. Prog. Phys., 52, 945

Kifonidis, K., Plewa, T., Janka, H.-Th. & E. Mueller 2003, A&A, submitted (astro-ph/0302239)

Langanke, K. & Martinez-Pinedo, G. 2000, Nucl. Phys. A, 673, 481

Mayle, R. & Wilson, J. R. 1988, ApJ, 334, 909

Meyer, B. S., McLaughlin, G. C., & Fuller, G. M. 1998, Phys. Rev. C, 58, 3696

Miyaji, S., Nomoto, K., Yokoi, K., & Sugimoto, D. 1980, PASJ, 32, 303

Miyaji, S. & Nomoto, K. 1987, ApJ, 318, 307

Nomoto, K., Sparks, W. M., Fesen, R. A., Gull, T. R., Miyaji, S., & Sugimoto, D. 1982, Nature, 299, 803

Nomoto, K. 1984, ApJ, 277, 791

Nomoto, K. 1987, ApJ, 322, 206

Nomoto, K. & Kondo, Y. 1991, ApJ, 367, L19

Otsuki, K., Tagoshi, H., Kajino, T., & Wanajo, S. 2000, ApJ, 533, 424

Qian, Y. -Z. & Woosley, S. E. 1996, ApJ, 471, 331

Qian, Y. -Z., Haxton, W. C., Langanke, K., & Vogel, P. 1997, Phys. Rev. C, 55, 1532

Qian, Y. -Z., Vogel, P., & Wasserburg, G. J. 1998, ApJ, 506, 868

Qian, Y. -Z. & Wasserburg, G. J. 2001, ApJ, 559, 925

Qian, Y. -Z. & Wasserburg, G. J. 2002, ApJ, 567, 515

Qian, Y. -Z. & Wasserburg, G. J. 2003, ApJ, in press (astro-ph/0301461)

Sato, K. 1974, Prog. Theor. Phys., 51, 726

Schatz, H., Toenjes, R., Kratz, K.-L., Pfeiffer, B., Beers, T.C., Cowan, J.J., & Hill, V. 2002, ApJ, 579, 626

Seeger, P. A. & Schramm, D. N. 1970, ApJ, 160, L157

Schramm, D. N. 1973, ApJ, 185, 293

Shen, H., Toki, H., Oyamatsu, K., & Sumiyoshi, K. 1998, Nucl. Phys. A, 637, 435

Sneden, C., McWilliam, A., Preston, G. W., Cowan, J. J., Burris, D. L., & Armosky, B. J. 1996, ApJ, 467, 819

Sneden, C., Cowan, J. J., Ivans, I. I., Fuller, G. M., Burles, S., Beers, T. C., Lawler, J. E. 2000, ApJ, 533, L139

Sneden, C. & Cowan, J. J. 2003, Science, 299, 70

Sneden, C., Cowan, J. J., Lawler, J. E., Ivans, I. I., Burles, S., Beers, T. C., Primas, F., Hill, V., Truran, J. W., Fuller, G. M., Pfeiffer, B., & Kratz, K. -L. 2003, ApJ, in press (astro-ph/0303542)

Sumiyoshi, K., Terasawa, M., Mathews, G. J., Kajino, T., Yamada, S., & Suzuki, H. 2001, ApJ, 562, 880

Surman, R. & Engel 2001, Phys. Rev. C, 64, 35801

Thompson, T. A., Burrows, A., & Meyer, B. S. 2001, ApJ, 562, 887

Thompson, T. A., Burrows, A., & Pinto, P. A. 2003, ApJ, in press (astro-ph/0211194)

Umeda, H. & Nomoto, K. 2002, ApJ, 565, 385

Umeda, H. & Nomoto, K. 2003, Nature, in press (astro-ph/0301315)

Utsunomiya, H., Yonezawa, Y., Akimune, H., Yamagata, T., Ohta, M., Fujishiro, M., Toyokawa, H., & Phgaki, H. 2001, Phys. Rev. C, 63, 18801

Wallerstein, G., Vanture, A. D., Jenkins, E. B., & Fuller, G. M. 1995, ApJ, 449, 688

Wanajo, S., Kajino, T., Mathews, G. J., & Otsuki, K. 2001, ApJ, 554, 578

Wanajo, S., Itoh, N., Ishimaru, Y., Nozawa, S., & Beers, T. C. 2002, ApJ, 577, 853

Wasserburg, G. J. & Qian, Y. -Z., 2000 ApJ, 529, L21

Wheeler, J. C., Cowan, J. J., & Hillebrandt, W. 1998, ApJ, 493, L101

Woosley, S. E. & Baron, E. 1992, ApJ, 391, 228

Woosley, S. E. & Hoffman, R. D. 1992, ApJ, 395, 202

Woosley, S. E., Wilson, J. R., Mathews, G. J., Hoffman, R. D., & Meyer, B. S. 1994, ApJ, 433, 229

Woosley, S. E. & Weaver, T. A. 1995, ApJS, 101, 181

Yamada, S. & Sato, K. 1994, ApJ, 434, 268

AAS LaTeX macros v5.0.

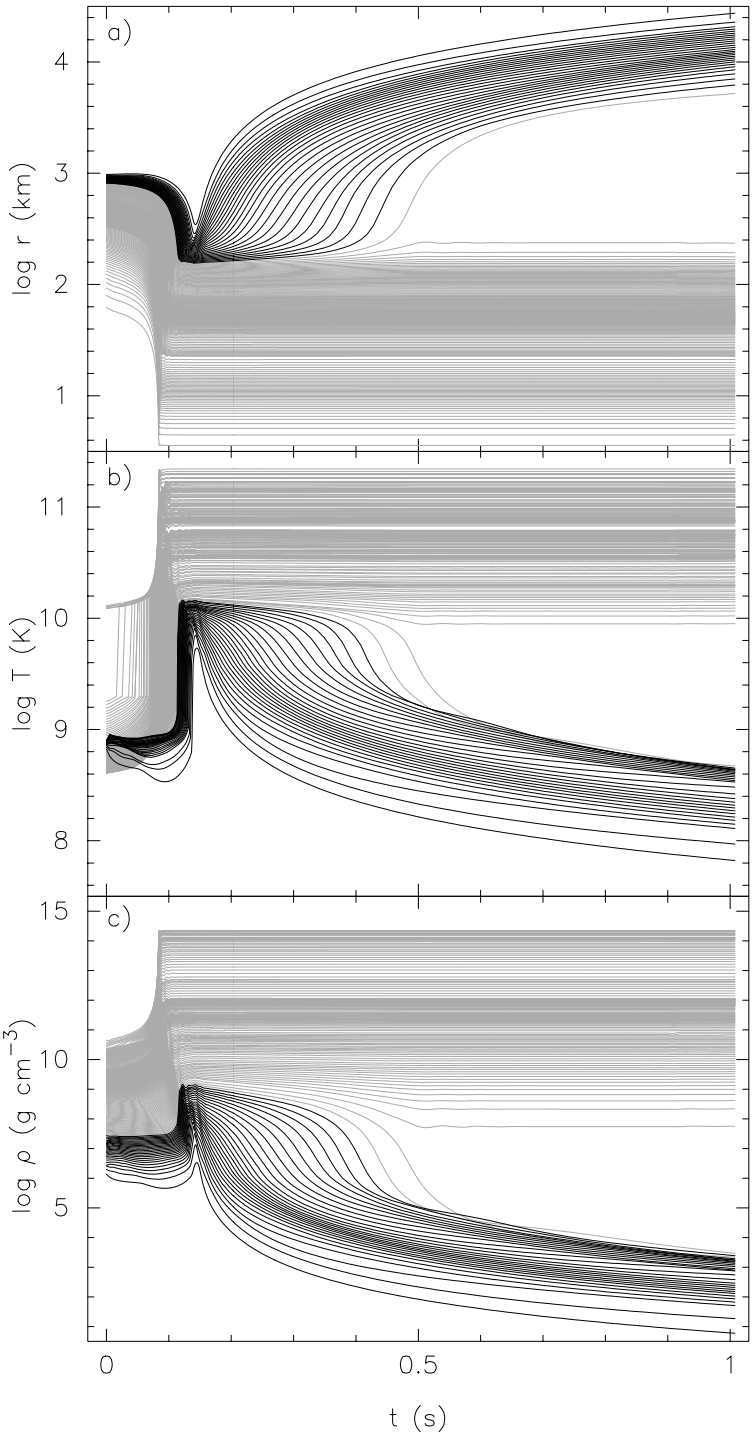

Fig. 1.— Time variations of (a) radius, (b) temperature, and (c) density for all mass points in the weak prompt explosion of a $9M_{\odot}$ star (model Q0). The ejected mass points are denoted in black, while those of the remnant are in grey.

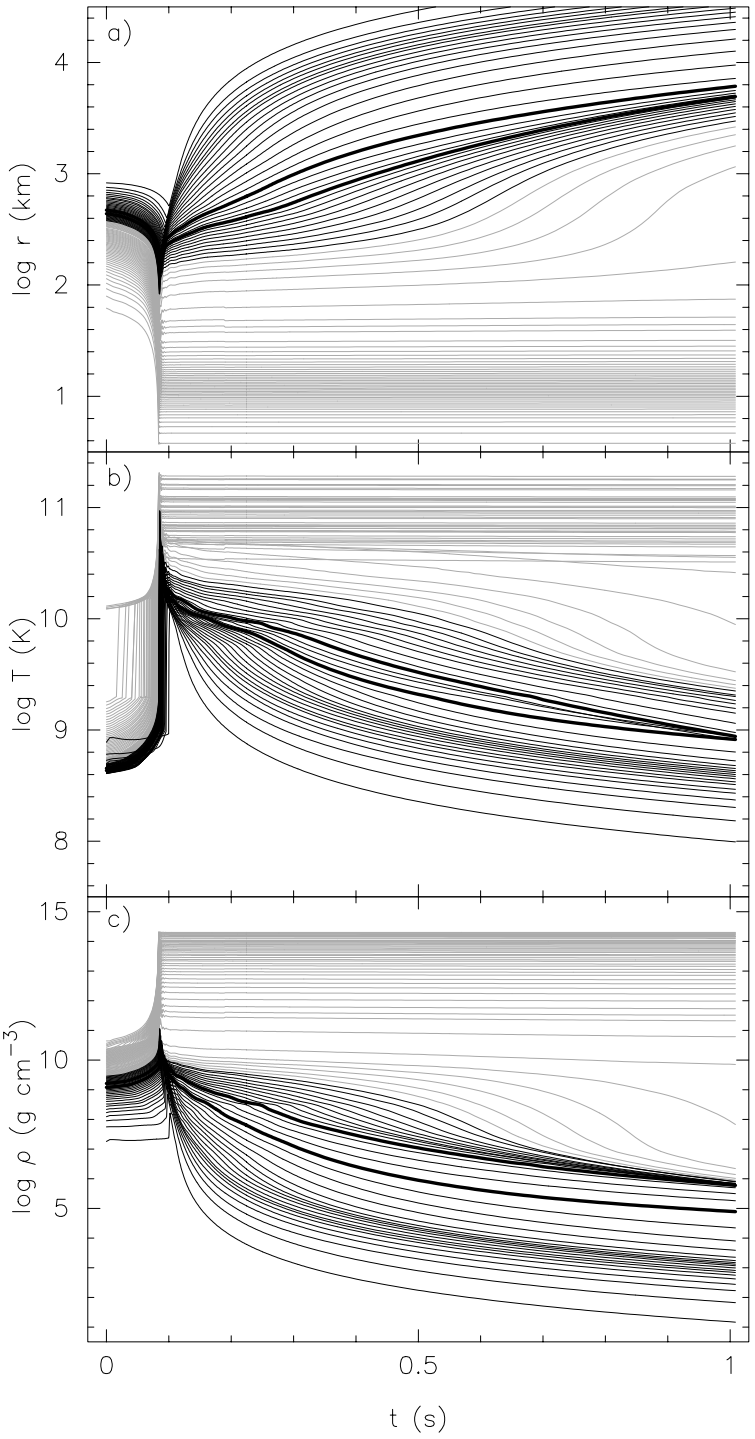

Fig. 2.— Time variations of (a) radius, (b) temperature, and (c) density for selected mass points (with roughly an equal mass interval) in the energetic prompt explosion of a $9M_{\odot}$ star, in which the shock-heating energy is enhanced artificially by a factor of 1.6 (model Q6). The ejected mass points are denoted in black, while those of the remnant are in grey. Thick lines denote the mass shells with $M_{\rm ej} = 0.2$ and $0.3M_{\odot}$ ($Y_e = 0.20$ and 0.14, respectively; see Figure 3). The material between these lines is particularly of importance to account for the solar r-process abundances (see discussion in § 3).

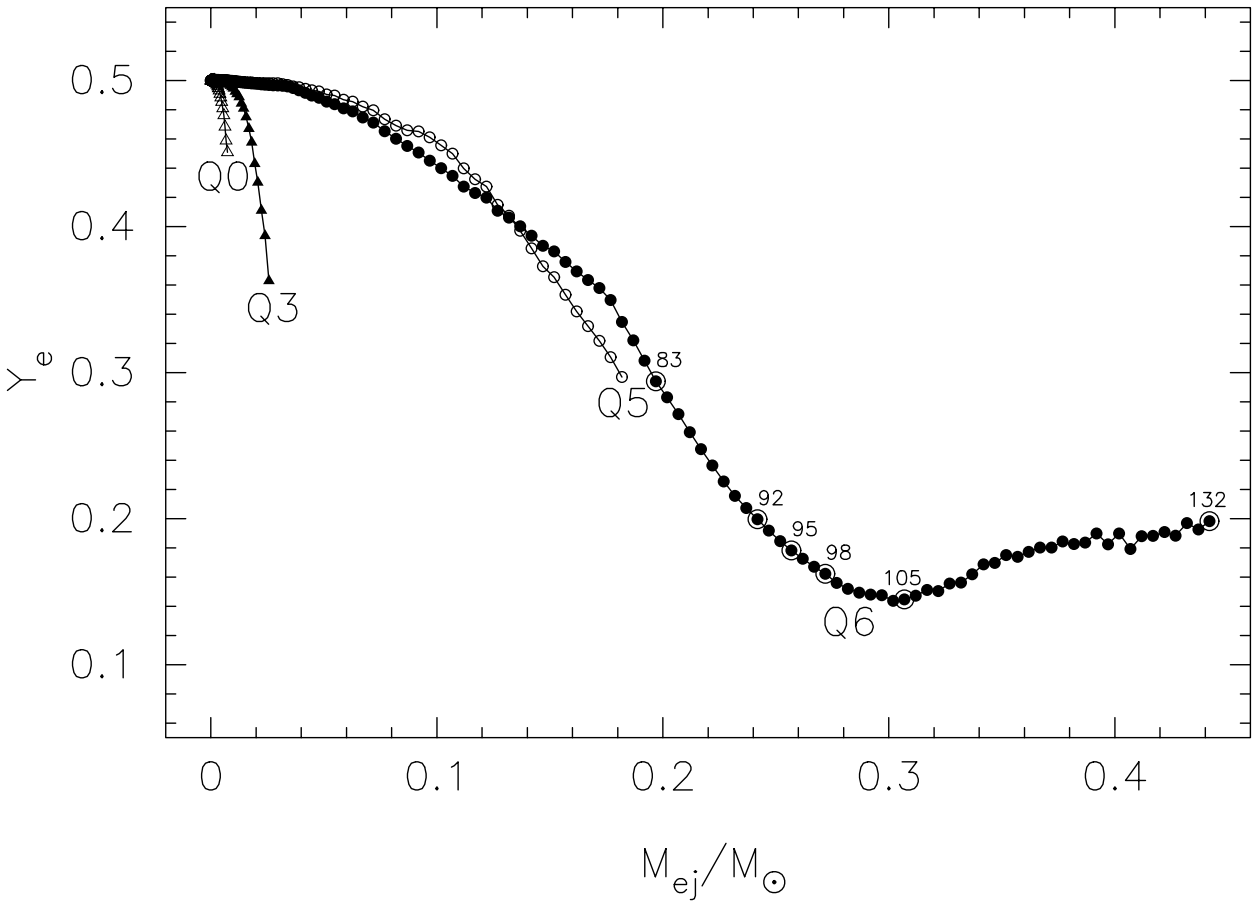

Fig. 3.— Y_e distribution in the ejected material in models Q0 (open triangles), Q3 (filled triangles), Q5 (open circles), and Q6 (filled circles). The surface of the O-Ne-Mg core is at mass coordinate zero. For model Q6, selected mass points are denoted by zone numbers (see Table 2).

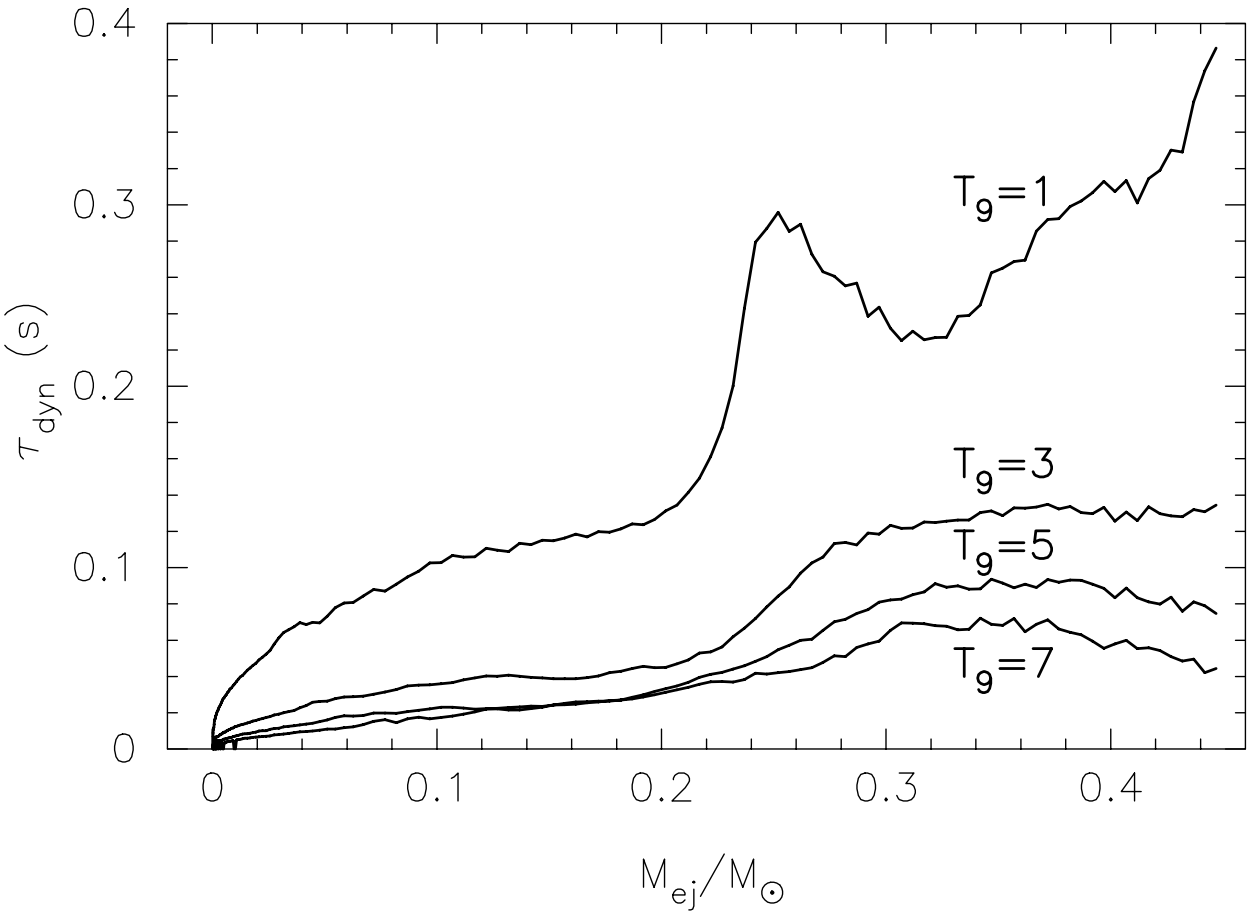

Fig. 4.— The dynamical timescales of the outgoing material as functions of $M_{\rm ej}$ at $T_9 = 1, 3, 5$, and 7 in model Q6.

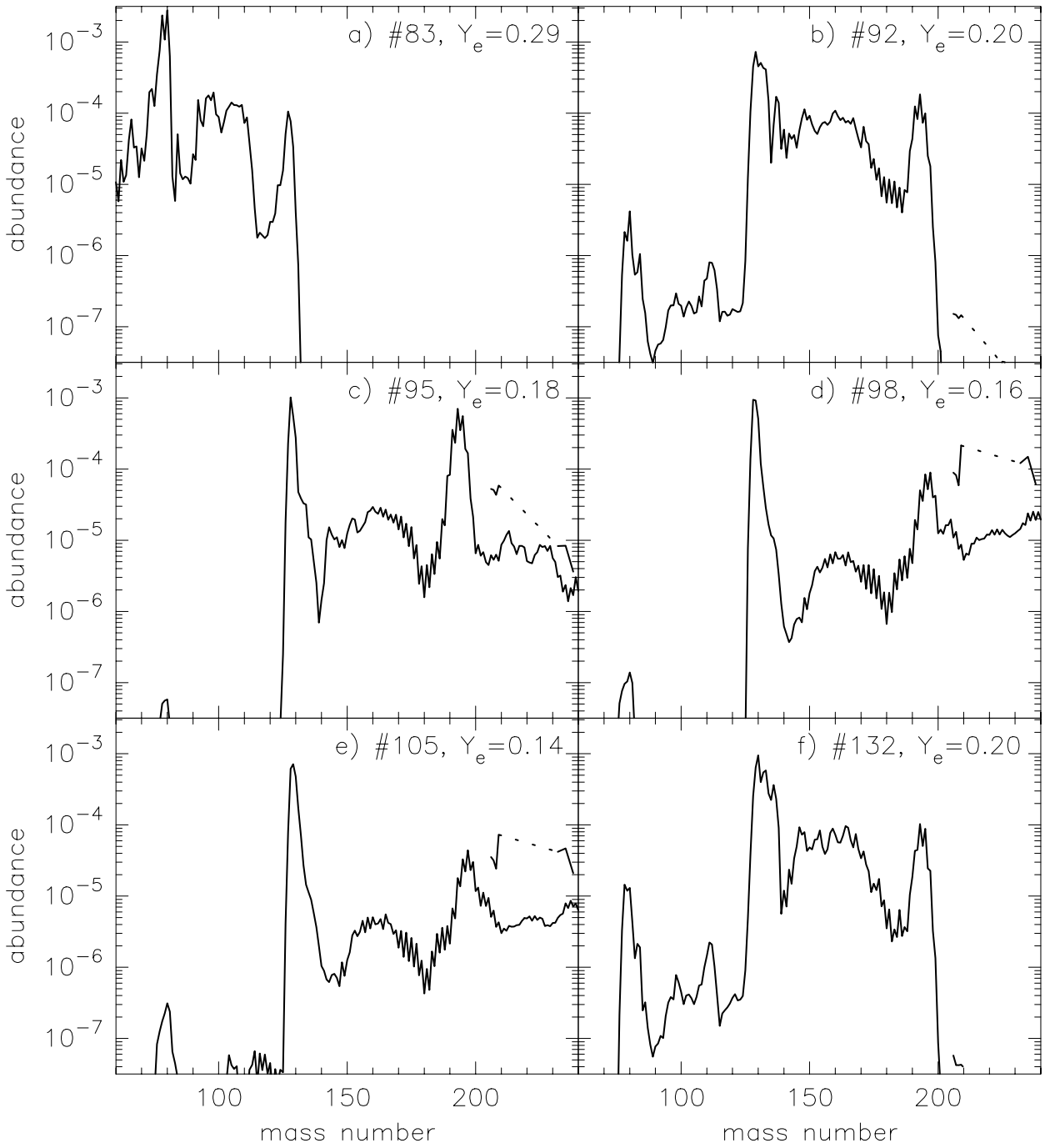

Fig. 5.— Final abundances as a function of mass number from r-process calculations for trajectories (a) 83, (b) 92, (c) 95, (d) 98, (e) 105, and (f) 132 in Table 2.

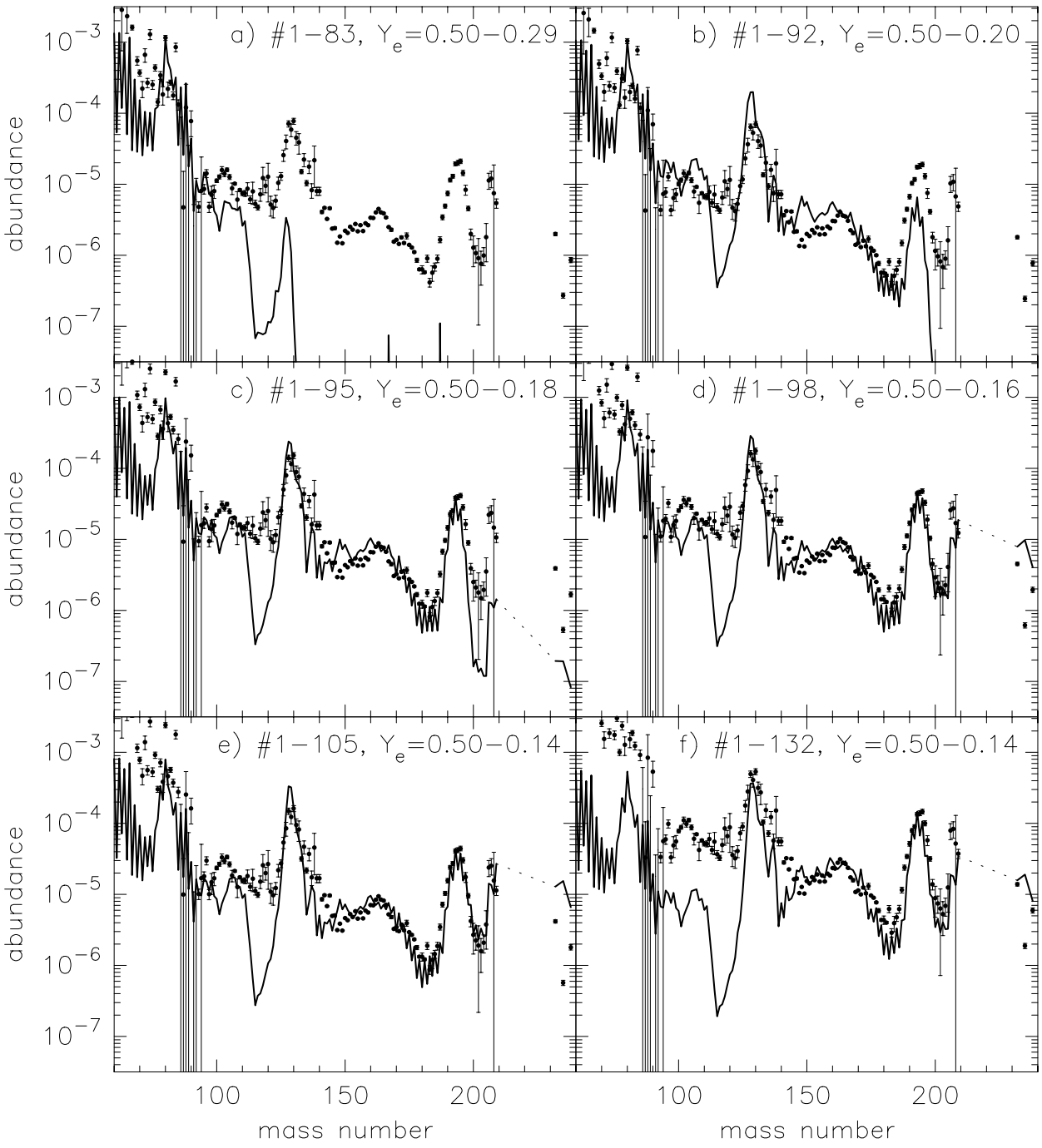

Fig. 6.— Final mass-averaged r-process abundances (line) as a function of mass number obtained from the ejected zones in (a) models Q6a, (b) Q6b, (c) Q6c, (d) Q6d, (e) Q6e, and (f) Q6f (see Table 2). These are compared with the solar r-process abundances (points) of Käppeler et al. (1989), which is scaled to match the height of the first peak ($A = 80$) for (a)-(b) and the third peak ($A = 195$) for (c)-(f).

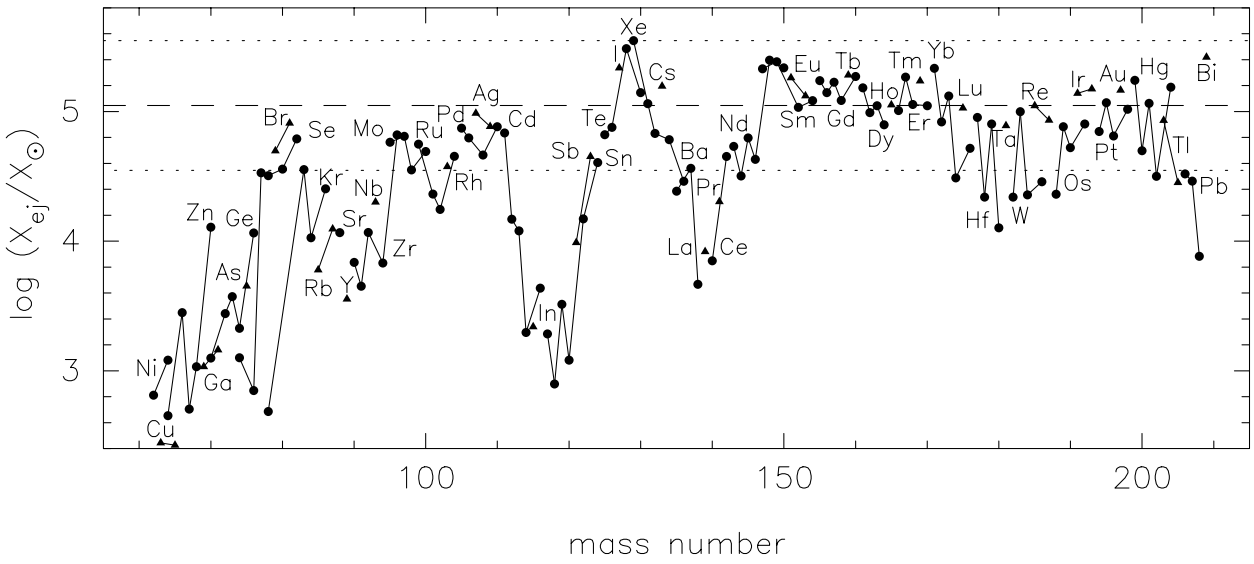

Fig. 7.— Mass-averaged production factors in model Q6e (see Table 2). Isotopes of a given element are connected by lines. Elements with even and odd atomic numbers are denoted by points and triangles, respectively. The dotted lines indicate a normalization band (see text), with its median value (dashed line).

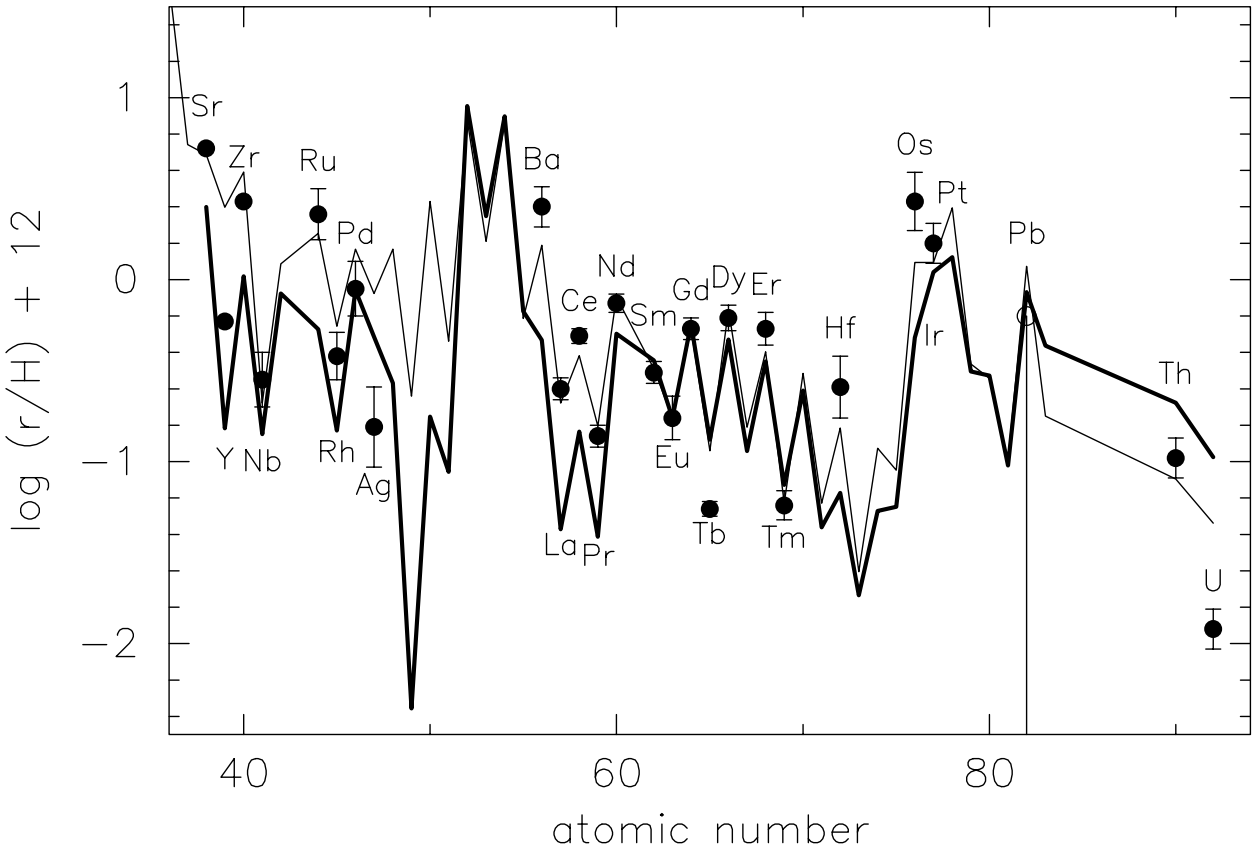

Fig. 8.— Comparison of the mass-integrated yields (thick line) for model Q6e, scaled at Eu ($Z = 63$), with the abundance pattern of CS 31082-001 (filled circles, with observational error bars), as a function of atomic number. For Pb, the observed upper limit is shown by the open circle. The scaled solar r-process pattern is shown by the thin line.

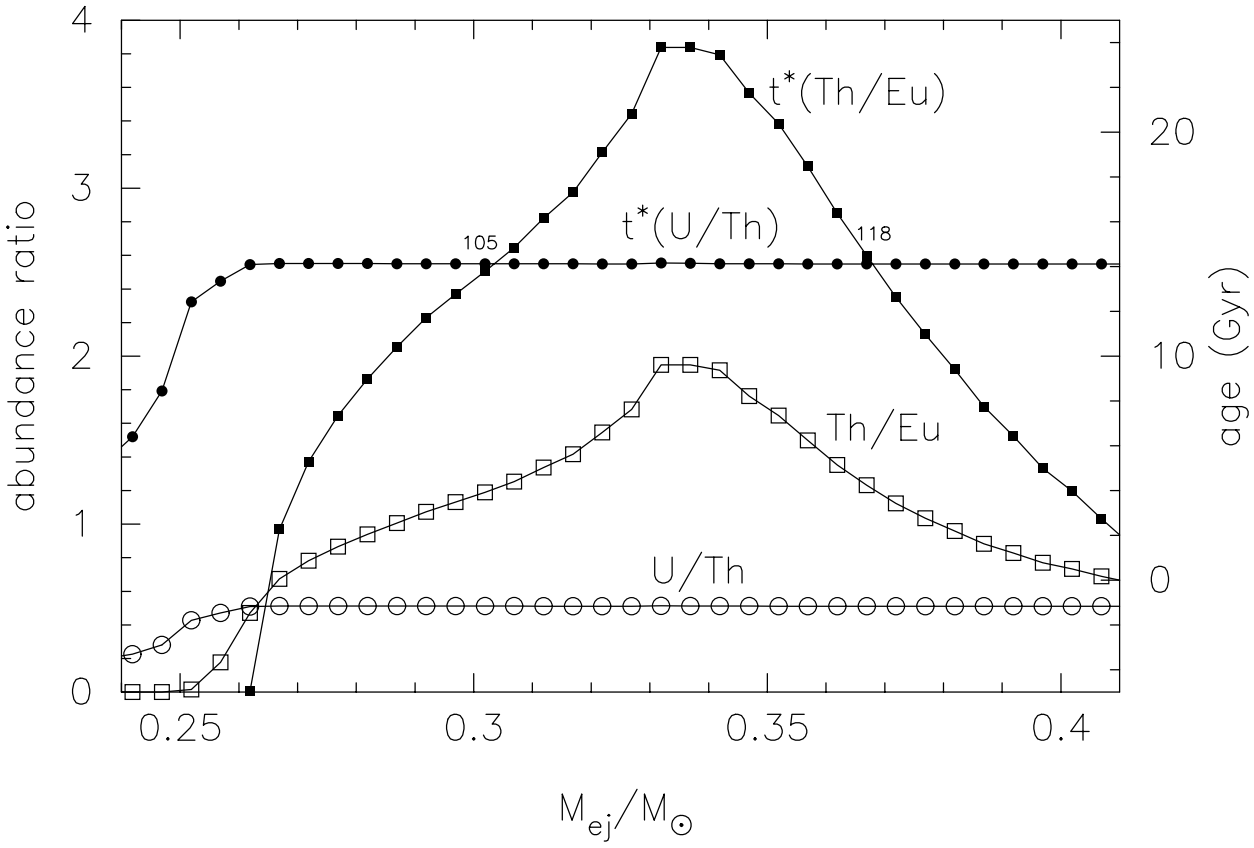

Fig. 9.— Mass-integrated abundance ratios Th/Eu (open squares) and U/Th (open circles) from the surface of the core to the mass point $M_{\rm ej}$ in model Q6. The surface of the O-Ne-Mg core is at mass coordinate zero. Ages of CS 31082-001 t^*(Th/Eu) (filled squares) and t^*(U/Th) (filled circles) inferred by these ratios are also shown. The lines of these ages have intersections near the mass points 105 and 118.